2014 IEEE International Conference on Robotics & Automation (ICRA)
Hong Kong Convention and Exhibition Center
May 31 - June 7, 2014. Hong Kong, China

Realization of Spring Loaded Inverted Pendulum Dynamics with a Two-link Manipulator based on the Bio-inspired Coordinate System

Sehoon Oh and Kyoungchul Kong

***Abstract*— In this paper, kinematics, statics, and dynamics of a two-link manipulator with a biarticular actuation mechanism are discussed. The biarticular actuation mechanism is inspired from the musculoskeletal structure of animals and is utilized in the controller design, as well as the mechanism design. For an effective and convenient expression of the equation of motion, the rotating coordinate system is adopted unlike the conventional robotic manipulators, the dynamics of which are obtained in the fixed coordinate system. It is proved in this paper that the biarticular actuation mechanism makes the control of the end-effector easier, more robust, and more intuitive than typical actuation mechanisms. Based on the derived equation of motion of a robotic manipulator in the rotating coordinate system, a disturbance-observer-based controller is proposed for realization of the Spring Loaded Inverted Pendulum (SLIP) model, which is a common model of human lower extremities but has seldom been realized in practice. The proposed methods are all verified by simulation studies in this paper.**

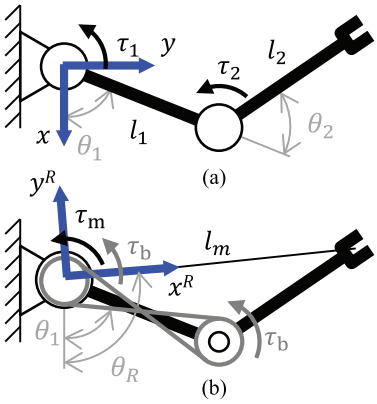

Fig. 1. Schematic of two-link robotic manipulators with (a) typical joint actuation mechanism and (b) biarticular actuation mechanism

I. Introduction

A number of efforts have been made to develop a new mechanism and control algorithm that can overcome the inherent limitations and difficulties of conventional robotic manipulators. In this aspect, inspiration from biology and nature often provides necessary and critical ideas for breaking through the limitations. For example, when the robots are desired to follow the human motions (or at least motion characteristics), the most intuitive and effective way of design may be following the musculoskeletal structure of the human body. Therefore, the bio-inspiration has become an important process in the design of mechanical, control, and mechatronic parts of robotic manipulators.

The major differences between the typical robotic manipulators and the human musculoskeletal structure include (1) the biarticular actuation mechanism[1], [2], and (2) the coordinate system that observes an end-effector. The biarticular actuation mechanism that enables unique distribution of actuation torques[3] has been intensively investigated by many researchers recently. Kumamoto *et al.* proposed a three-pair six-muscle structure as a basic actuator model of a two-link manipulator inspired from the human's musculoskeletal structure; he showed how the biarticular muscles co-work to generate hand forces with clinical tests. The joint torque generation model in the biarticular actuation mechanism was quasi-statically analyzed in [4]. The proposed algorithm was found to be optimal in terms of the ∞–norm of the muscular forces required to generate the hand forces[5]. The biarticular actuation mechanism is being widely adopted in biomimetic robots for jumping and running[6], [7]. Such robots adopted the biarticular actuation mechanism to improve the jumping stability and performance, the theoretical background of which is shown in [8].

In spite of such a new paradigm of the bio-inspired robotics, most of the methodologies for obtaining the equations of motion and for analyzing dynamics still follow the conventional way of dynamic systems. For the sake of simplicity in the derivation of the equations of motion, the whole body motion is usually regarded as a combination of joint motions, where each body segment is treated all separately. In many cases, actuators are installed at each joint, and thus the control input is applied to each joint. Although the most of the robotic joints are pinned joints that rotate around fixed axes, the whole body motion is usually described in the Cartesian coordinate system with a fixed reference frame in order to make it intuitive to observe the position of an end-effector from the viewpoint of a human operator.

The bio-inspired robotic manipulators, however, should be described in a coordinate system that is more compatible with the biological system, i.e., so-called the bio-inspired coordinate system. One example is shown in Fig. 1. In the typical robotic manipulators, the position of an end-effector is measured from an independent reference frame, i.e., the Cartesian coordinate system fixed outside of the robot system[9], [10] (see Fig. 1(a)). On the other hand, in the human motion control the hand or foot is seen in the rotating coordinate system, in which the origin is at the

This work was supported by the National Research Foundation of Korea(NRF) grant funded by the Korea government(MSIP) (NRF-2012R1A1A1008271).

The authors are with Department of Mechanical Engineering, Sogang University Seoul, Korea e-mail: {sehoon74, kckong}@sogang.ac.kr

most proximal joint of the manipulator and the reference frame is rotated along the position of the most distal joint of the manipulator (see Fig. 1(b)). The spring-loaded inverted pendulum (SLIP) model[11], [12], [13] which is considered as a potential and effective model of human walking and running can be described the most appropriately in this rotating coordinate system; the motion of an end-effector is expressed in the rotating coordinate system in the SLIP model.

In this paper, the configuration of a two-link robotic manipulator is designed to have the biarticular actuation mechanism and controlled in the rotating coordinate system to realize the SLIP dynamics. There are a few applications of the biarticular actuation theory[14], such as robots for jumping and swimming[8], [15]. These systems, however, were designed only for the selected movement and performance. In this paper, more fundamental information on the biarticular actuation mechanism and its dynamics, including kinematics and statics, are introduced, and it is proved that the use of the bio-inspired coordinate system (i.e., the rotating coordinate system) simplifies the expression of the kinematics and dynamics of a biarticular actuation mechanism.

In addition, a control algorithm is developed based on the proposed biarticular actuation mechanism and the rotating coordinate system in order to realize the SLIP motion. A feedback controller is designed based on the equation of motion in the rotating coordinate system. In particular, a disturbance-observer(DOB)-based feedback controller[16] that decouples the x and y axes motions in the rotating coordinate system is designed for verification of the effectiveness of the proposed mechanism and analysis method. This decoupling enables the realization of the SLIP dynamics with a two-link robotic manipulator, which has been remained as a challenging problem in robotics[7], [12], [13].

II. Kinematics and Statics in the Rotating Coordinate System

A. Introduction of the Rotating Coordinate System

Figure 1 shows the schematics of robotic manipulators with and without the biarticular actuation mechanism. In the figure, the two different coordinate systems are also shown; the conventional fixed coordinate system in Fig. 1(a) and the rotating coordinate system in Fig. 1(b). In the rotating coordinate system, the x^R axis is set along the line connecting the first joint and the end-effector, and the y^R axis is set orthogonal to the x^R axis. Since the end-effector is not fixed, the coordinate system is not fixed also; it rotates along the rotation of the end-effector. This is the rotating coordinate system proposed in this paper to analyze the motion of a two-link manipulator in a bio-inspired way.

The parameters, l_1, l_2, are respectively the lengths of the first and second links, θ_1 is the angle of the first link in the fixed coordinate system, and θ_2 is the relative angle between the first and the second links. θ_R is the angle between the reference frames of the fixed and rotating coordinate systems.

B. Kinematics in the Rotating Coordinate System

For the sake of simplicity in the kinematic analysis of a biarticularly-actuated two-link manipulator with the proposed rotating coordinate system, the two length parameters, l_1 and l_2, are assumed to be identical, which may be a practical assumption in many robotic manipulators. Even for the cases without this assumption, the proposed method can be applied without any modification, but the equations become lengthier.

The joint angular velocity $[\dot{\theta}_1\, \dot{\theta}_2]^T \in \mathbb{R}^2$ can be presented by $[\dot{\theta}_1\, \dot{\theta}_{12}]^T \in \mathbb{R}^2$ by a linear transformation:

$$\begin{bmatrix} 1 & 0 \\ 1 & 1 \end{bmatrix} \begin{bmatrix} \dot{\theta}_1 \\ \dot{\theta}_2 \end{bmatrix} = \begin{bmatrix} \dot{\theta}_1 \\ \dot{\theta}_1 + \dot{\theta}_2 \end{bmatrix} =: \begin{bmatrix} \dot{\theta}_1 \\ \dot{\theta}_{12} \end{bmatrix}, \tag{1}$$

where θ_{12} represents $(\theta_1 + \theta_2)$. In this paper, $\dot{\theta}_{12}$ is considered the velocity output that corresponds to the biarticular muscle torque input [14].

The velocity of the end-effector in the Cartesian coordinate system is transformed to the velocity in the rotating coordinate system as follows.

$$\begin{bmatrix} \dot{x}^R \\ \dot{y}^R \end{bmatrix} = \begin{bmatrix} \cos\theta_R & \sin\theta_R \\ -\sin\theta_R & \cos\theta_R \end{bmatrix} \begin{bmatrix} \dot{x} \\ \dot{y} \end{bmatrix} \tag{2}$$

Based on the geometry in Fig. 1, θ_R becomes $(\theta_1 + \frac{\theta_2}{2})$ with the assumption of $l_1 = l_2$.

Equations (1) and (2) transform the conventional kinematic relationship between $[\dot{x}\, \dot{y}]^T \in \mathbb{R}^2$ and $[\dot{\theta}_1\, \dot{\theta}_2]^T$ to a new kinematic relationship, which is between $[\dot{x}^R\, \dot{y}^R]^T \in \mathbb{R}^2$ and $[\dot{\theta}_1\, \dot{\theta}_{12}]^T$, i.e.,

$$\begin{bmatrix} \dot{x}^R \\ \dot{y}^R \end{bmatrix} = l \begin{bmatrix} \sin\frac{\theta_2}{2} & -\sin\frac{\theta_2}{2} \\ \cos\frac{\theta_2}{2} & \cos\frac{\theta_2}{2} \end{bmatrix} \begin{bmatrix} \dot{\theta}_1 \\ \dot{\theta}_{12} \end{bmatrix} = J_R \begin{bmatrix} \dot{\theta}_1 \\ \dot{\theta}_{12} \end{bmatrix}, \tag{3}$$

where J_R is a new Jacobian that relates the end-effector velocity in the rotating coordinate system (i.e., $[\dot{x}^R\, \dot{y}^R]^T \in \mathbb{R}^2$) and the angular velocity of the biarticular actuator coordination (i.e., $[\dot{\theta}_1\, \dot{\theta}_{12}]^T$). Based on this kinematics, the inverse kinematics is derived as

$$\begin{bmatrix} \dot{\theta}_1 \\ \dot{\theta}_{12} \end{bmatrix} = J_R^{-1} \begin{bmatrix} \dot{x}^R \\ \dot{y}^R \end{bmatrix} = \frac{1}{l \sin\theta_2} \begin{bmatrix} \cos\frac{\theta_2}{2} & \sin\frac{\theta_2}{2} \\ -\cos\frac{\theta_2}{2} & \sin\frac{\theta_2}{2} \end{bmatrix} \begin{bmatrix} \dot{x}^R \\ \dot{y}^R \end{bmatrix} \tag{4}$$

Equations (3) and (4) are the forward and inverse kinematics of the two-link manipulator with the biarticular actuation mechanism represented in the rotating coordinate system.

C. Statics Based on the Proposed Kinematics

Biarticular muscle/actuator torque input, τ_b which works as an input acting on the two joints simultaneously[14], and the monoarticular torque, τ_m which works only on the first joint, are defined the torque inputs in the proposed bio-inspired coordinate system. The following equation relates the conventional torque inputs, τ_1 and τ_2, which are the independent joint torque inputs, to a new set of torques, τ_m and τ_b.

$$\begin{bmatrix} \tau_1 \\ \tau_2 \end{bmatrix} = \begin{bmatrix} 1 & 1 \\ 0 & 1 \end{bmatrix} \begin{bmatrix} \tau_m \\ \tau_b \end{bmatrix} = \begin{bmatrix} \tau_m + \tau_b \\ \tau_b \end{bmatrix} \tag{5}$$

The forces at the end-effector $[f_x\ f_y]^T \in \mathbb{R}^2$ defined in the fixed coordinate system can be transformed to $[f_x^R\ f_y^R]^T \in \mathbb{R}^2$ in the rotating coordinate system as

$$\begin{bmatrix} f_x \\ f_y \end{bmatrix} = \begin{bmatrix} \cos\theta_R & -\sin\theta_R \\ \sin\theta_R & \cos\theta_R \end{bmatrix} \begin{bmatrix} f_x^R \\ f_y^R \end{bmatrix} \tag{6}$$

Equations (5) and (6) with the assumption of $l_1 = l_2 = l$ provide the simplified statics between the input torques and the output forces at the end-effector as follows.

$$\begin{bmatrix} \tau_m \\ \tau_b \end{bmatrix} = l \begin{bmatrix} \sin\frac{\theta_2}{2} & \cos\frac{\theta_2}{2} \\ -\sin\frac{\theta_2}{2} & \cos\frac{\theta_2}{2} \end{bmatrix} \begin{bmatrix} f_x^R \\ f_y^R \end{bmatrix} = J_R^T \begin{bmatrix} f_x^R \\ f_y^R \end{bmatrix} \tag{7}$$

The inverse statics can also be re-derived in the rotating coordinate system as

$$\begin{bmatrix} f_x^R \\ f_y^R \end{bmatrix} = \left(J_R^T\right)^{-1} \begin{bmatrix} \tau_m \\ \tau_b \end{bmatrix} = \frac{1}{2} \begin{bmatrix} \frac{(\tau_m - \tau_b)}{l \sin\frac{\theta_2}{2}} \\ \frac{(\tau_m + \tau_b)}{l \cos\frac{\theta_2}{2}} \end{bmatrix} \tag{8}$$

Note that the force acting on the end-effector along the x^R and y^R axes are also described by a common mode and a differential mode; $(\tau_m - \tau_b)$ determines f_x^R with a scale factor of $\frac{1}{2l \sin\theta_2/2}$, and $(\tau_m + \tau_b)$ determines f_y^R with a scale factor of $\frac{1}{2l \cos\theta_2/2}$. More detailed derivations of these equations can be found in our previous paper[17].

III. Design of Rotating-coordinated Workspace Disturbance Observer

Even though the torques can generate forces at the end-effector in the x^R and y^R directions independently by the proposed statics, it is not simple to control the two-link manipulator to behave as a SLIP model, since it has a different inertia structure. The inertia matrix is different between the two-link manipulator and the SLIP dynamic model; there is a coupling in the two-link manipulator between the inertias in the x^R direction and the y^R direction so that the actuation force in one direction will affect the acceleration in another direction.

A disturbance observer that can decouple the inertia structure to make a two-link manipulator behave as a SLIP model is proposed in this section. In order to design the observer, the dynamics is re-described in the rotating coordinate system of the biarticular actuation structure. Based on the derived dynamics, the disturbance observer is designed to decouple the inertia matrix.

A. Inertia Coupling Problem in Two-Link Manipulators

Equation (9) is the conventional description of the dynamics of a two-link manipulator, where τ_1 and τ_2 are the two torque inputs, and $\ddot{\theta}_1$ and $\ddot{\theta}_2$ are the acceleration outputs. g is the acceleration of gravity, d_i is the distance from the center of a joint i to the center of the gravity point of the link i, m_i is the weight of the link i, and J_i is the moment of inertia about an axis through the center of mass of link i.

$$\begin{aligned} &\begin{bmatrix} J_1+J_2+m_2l_1^2+2m_2l_1d_2\cos\theta_2 & J_2+m_2l_1d_2\cos\theta_2 \\ J_2+m_2l_1d_2\cos\theta_2 & J_2 \end{bmatrix} \begin{bmatrix} \ddot{\theta}_1 \\ \ddot{\theta}_2 \end{bmatrix} \\ &\quad + \begin{bmatrix} -m_2l_1d_2\sin\theta_2(\dot{\theta}_2^2 + 2\dot{\theta}_1\dot{\theta}_2) \\ m_2l_1d_2\sin\theta_2\dot{\theta}_1^2 \end{bmatrix} \\ &\quad + \begin{bmatrix} g(m_1d_1+m_2l_1)\cos\theta_1 + gm_2d_2\cos(\theta_1+\theta_2) \\ gm_2d_2\cos(\theta_1+\theta_2) \end{bmatrix} \\ &= \begin{bmatrix} \tau_1 \\ \tau_2 \end{bmatrix} \end{aligned} \tag{9}$$

This dynamic equation can be re-described in the proposed bio-inspired coordinate system using the following transformations:

$$\begin{bmatrix} \theta_1 \\ \theta_{12} \end{bmatrix} = \begin{bmatrix} 1 & 0 \\ 1 & 1 \end{bmatrix} \begin{bmatrix} \theta_1 \\ \theta_2 \end{bmatrix}, \quad \begin{bmatrix} \theta_1 \\ \theta_2 \end{bmatrix} = \begin{bmatrix} 1 & 0 \\ -1 & 1 \end{bmatrix} \begin{bmatrix} \theta_1 \\ \theta_{12} \end{bmatrix} \tag{10}$$

$$\begin{bmatrix} \tau_1 \\ \tau_2 \end{bmatrix} = \begin{bmatrix} 1 & 1 \\ 0 & 1 \end{bmatrix} \begin{bmatrix} \tau_m \\ \tau_b \end{bmatrix}, \quad \begin{bmatrix} \tau_m \\ \tau_b \end{bmatrix} = \begin{bmatrix} 1 & -1 \\ 0 & 1 \end{bmatrix} \begin{bmatrix} \tau_1 \\ \tau_2 \end{bmatrix} \tag{11}$$

With these relationships, the dynamics in (9) can be transformed as follows.

$$\begin{aligned} \begin{bmatrix} \tau_m \\ \tau_b \end{bmatrix} &= \begin{bmatrix} J_1 + m_2l_1^2 & m_2l_1d_2\cos\theta_2 \\ m_2l_1d_2\cos\theta_2 & J_2 \end{bmatrix} \begin{bmatrix} \ddot{\theta}_1 \\ \ddot{\theta}_{12} \end{bmatrix} \\ &\quad + \begin{bmatrix} -m_2l_1d_2\sin\theta_2\dot{\theta}_{12}^2 \\ m_2l_1d_2\sin\theta_2\dot{\theta}_1^2 \end{bmatrix} + \begin{bmatrix} g(m_1d_1+m_2l_1)\cos\theta_1 \\ gm_2d_2\cos\theta_{12} \end{bmatrix} \end{aligned} \tag{12}$$

This dynamic equations can be further transformed to describe the dynamics in the rotating coordinate system using the inverse kinematics in (4) and the inverse statics in (8), and a new operational inertia matrix in the rotating coordinate system can be derived as

$$\Lambda^R = \frac{1}{4l^2} \begin{bmatrix} \frac{J_1^R}{\sin^2\frac{\theta_2}{2}} & \frac{J_m^R}{\sin\theta_2} \\ \frac{J_m^R}{\sin\theta_2} & \frac{J_2^R}{\cos^2\frac{\theta_2}{2}} \end{bmatrix}, \tag{13}$$

where the inertia elements are defined as follows.

$$\begin{aligned} J_1^R &:= J_1 + m_2l^2 + J_2 - 2m_2d_2l\cos\theta_2 \\ J_2^R &:= J_1 + m_2l^2 + J_2 + 2m_2d_2l\cos\theta_2 \\ J_m^R &:= J_1 + m_2l^2 - J_2 \end{aligned} \tag{14}$$

Notice that J_m^R is the coupling inertia term that makes the motions in the x^R and y^R directions mutually dependent. Notice that if J_m^R is zero, there is no off-diagonal terms in (13).

B. Design of Rotating-coordinated Workspace Disturbance Observer

The coupling inertia term, i.e., J_m^R in (14), should be eliminated for a two-link manipulator to behave as this SLIP model, such that the external force applied in the x^R does not affect the motion in the y^R direction. For this purpose, a disturbance observer is designed in the rotating coordinate system to cancel this inertia coupling.

Equation (15) is the design of the proposed disturbance observer, where the disturbances, the control input and the system output are defined in the rotating coordinate system.

$$\begin{bmatrix} \hat{d}_x^R \\ \hat{d}_y^R \end{bmatrix} = Q(s)\left(\begin{bmatrix} u_x^R \\ u_y^R \end{bmatrix} - \Lambda_n^R \begin{bmatrix} \ddot{x}^R \\ \ddot{y}^R \end{bmatrix}\right), \quad (15)$$

where $Q(s)$ is a lowpass filter that determines the bandwidth of the overall disturbance observer. The signals, $u_\bullet^R$, $\ddot{x}^R$, $\ddot{y}^R$, $\hat{d}_\bullet^R$, etc., are all in the Laplace domain.

The proposed disturbance observer is named a *rotating-coordinated workspace disturbance observer* (RWDOB) in this paper, since it is designed in the rotating coordinate system of a biarticular actuation structure. The Workspace Disturbance Observer in [18] is a similar disturbance observer design, but it was designed in the conventional fixed coordinate system unlike the proposed algorithm.

In order to implement the proposed observer, the control inputs to the manipulator (i.e., u_x^R and u_y^R) and the transformed outputs of the end-effector (i.e., $\ddot{x}^R$ and $\ddot{y}^R$) need to be replaced by the actuator torques (i.e., τ_m and τ_b) and the measurements (i.e., $\ddot{\theta}_1$ and $\ddot{\theta}_{12}$). In this aspect, the proposed RCDOB in an implementable form is

$$\begin{bmatrix} \hat{d}_x^R \\ \hat{d}_y^R \end{bmatrix} = Q(s)\left((J_R^T)^{-1}\begin{bmatrix} \tau_m \\ \tau_b \end{bmatrix} - \Lambda_n^R J_R \begin{bmatrix} \ddot{\theta}_1 \\ \ddot{\theta}_{12} \end{bmatrix}\right) \quad (16)$$

To reject the coupling inertia (i.e., J_m^R), Λ_n^R in (16) is set as in (17) so that the coupling is treated as a disturbance to be eliminated by the feedback of the lumped disturbance.

$$\Lambda_n^R = \begin{bmatrix} \Lambda_{11_n}^R & 0 \\ 0 & \Lambda_{22_n}^R \end{bmatrix}, \quad (17)$$

where $\Lambda_{11_n}^R = \frac{J_{1n}^R}{4l^2 \sin^2 \frac{\theta_2}{2}}$ and $\Lambda_{22_n}^R = \frac{J_{2n}^R}{4l^2 \cos^2 \frac{\theta_2}{2}}$. With this decoupled nominal inertia matrix, J_R^T and J_R defined in (3) and (7), the RWDOB in (16) is organized as follows.

$$\begin{bmatrix} \hat{d}_x^R \\ \hat{d}_y^R \end{bmatrix} = \frac{Q(s)}{2l}\left(\begin{bmatrix} \frac{1}{\sin\frac{\theta_2}{2}}(\tau_m - \tau_b) \\ \frac{1}{\cos\frac{\theta_2}{2}}(\tau_m + \tau_b) \end{bmatrix} - \begin{bmatrix} \frac{J_1^R}{2\sin\frac{\theta_2}{2}}\left(\ddot{\theta}_1 - \ddot{\theta}_{12}\right) \\ \frac{J_2^R}{2\cos\frac{\theta_2}{2}}\left(\ddot{\theta}_1 + \ddot{\theta}_{12}\right) \end{bmatrix}\right) \quad (18)$$

Lastly, the estimated disturbances in the rotating coordinate system (i.e., $[\hat{d}_x^R\ \hat{d}_y^R]^T$) should be transformed to the coordinate system of actual actuators so that they can be fed back into the actuators, i.e.

$$\begin{aligned} \begin{bmatrix} \hat{d}_m^R \\ \hat{d}_b^R \end{bmatrix} &= J_R^T \begin{bmatrix} \hat{d}_x^R \\ \hat{d}_y^R \end{bmatrix} \\ &= \frac{Q(s)}{2}\left(\begin{bmatrix} (\tau_m - \tau_b) + (\tau_m + \tau_b) \\ -(\tau_m - \tau_b) + (\tau_m + \tau_b) \end{bmatrix} \right. \\ &\quad \left. - \begin{bmatrix} \frac{J_1^R}{2}\left(\ddot{\theta}_1 - \ddot{\theta}_{12}\right) + \frac{J_2^R}{2}\left(\ddot{\theta}_1 + \ddot{\theta}_{12}\right) \\ -\frac{J_1^R}{2}\left(\ddot{\theta}_1 - \ddot{\theta}_{12}\right) + \frac{J_2^R}{2}\left(\ddot{\theta}_1 + \ddot{\theta}_{12}\right) \end{bmatrix}\right) \quad (19) \end{aligned}$$

The transformation in (19) cancels out $\sin\frac{\theta_2}{2}$ and $\cos\frac{\theta_2}{2}$ terms of the denominators in (18), and this is the final design of the proposed RWDOB. Notice that there is no division by $\sin\theta_2$ or $\cos\theta_2$ that may cause a singularity problem.

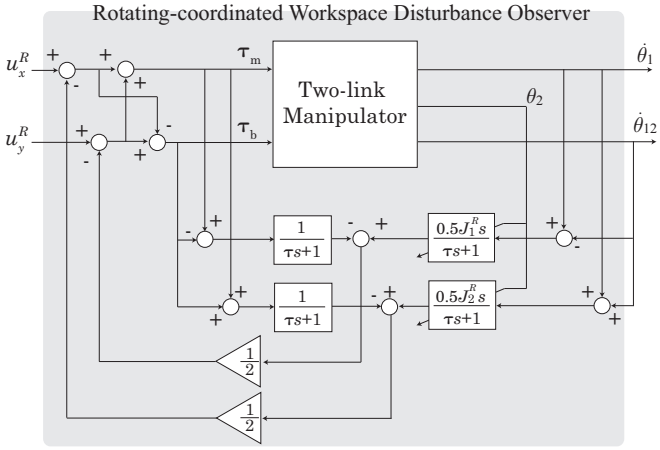

Fig. 2. The proposed control algorithm with the Rotating-coordinated Workspace Disturbance Observer

The design of the proposed RWDOB is illustrated as the shaded area of Fig. 2, where $Q(s)$ is set to a lowpass filter with a time constant of τ (i.e., $Q(s) = \frac{1}{\tau s+1}$). The only time varying component in this design is the nominal inertias which involve the joint angle, θ_2, in the numerators.

Notice that the RWDOB is a feedback compensator that rejects the undesired term (i.e., the coupled inertia term) only. For achieving the other control objectives, such as tracking performance, robust stability, and so on, an additional feedback control algorithm may be necessary on top of the proposed algorithm, e.g., the nonlinear and gravitational terms in the dynamics can be compensated for using the computed torque algorithm, and any additional feedback control for reference tracking can be added to u_x^R and u_y^R in Fig. 2.

IV. Realization of SLIP Dynamic Model by the RWDOB

To evaluate the decoupling performance of the proposed RWDOB for a two-link biarticularly-actuated manipulator, simulation studies on the collision of an end-effector were carried out. As explained previously, the motion of the end-effector generated by reaction against the external forces, which is a mechanical property called the impedance, is a significant aspect in the realization of the SLIP dynamic model; the effect of the coupling inertia should be removed not only with respect to the control input force but also with regard to the external force.

When a force is applied at the end-effector of a SLIP dynamic model in the x^R direction in Fig. 3, the end-effector is supposed to generate movements only in the x^R direction. For a two-link manipulator to exhibit the SLIP model dynamics, the end-effector of a two-link manipulator should make such movements against the exogenous forces in the same x^R direction, which is usually not the case in typical two-link manipulators due to the coupling inertia.

It should be noted that the proposed RWDOB can remove this coupling effect and control the way of reaction against the external force in the x^R and y^R directions independently. In order to verify this feature, a controller consisting of the

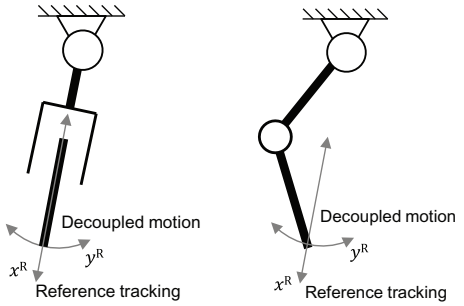

Fig. 3. Realization of SLIP model dynamics (left) by a two-link manipulator (right)

TABLE I
PARAMETER OF SIMULATION

m_1	2.64 kg	l_1	0.3 m	d_1	0.15 m	J_1	0.0853 kg·m^2
m_2	2.64 kg	l_2	0.3 m	d_2	0.15m	J_2	0.0853 kg·m^2
θ_1^0	$\pi/4$	θ_2^0	$-\pi/2$				

proposed RWDOB is designed as in Fig. 2 with an additional velocity feedback controller designed on u_x^R and u_y^R. The parameters used in the simulation are shown in Table I.

An impact force was generated by a collision in the x^R direction, and the reaction of the end-effector was examined to verify the controlled (i.e., decoupled) reaction force. The disturbance observer loop for the x^R direction was suppressed to make the impedance in the x^R direction low, while the RWDOB in the y^R direction was activated to impose a high impedance in that direction. Note that the back-drivability and torque-mode control of the actuators are assumed in the simulations.

In order to emphasize the effectiveness of the proposed algorithm, another type of the disturbance observer previously proposed in [19] was also applied and compared with the proposed algorithm. In [19], two separate disturbance observers were implemented onto two joints, which is a similar configuration to the proposed controller design. However, the disturbance observers in [19] were designed in the coordinate system defined on the joint space without taking into consideration the whole dynamics of the two-link manipulator and the characteristics of a biarticular actuation mechanism, and therefore this disturbance observer may not be able to adjust the impedance in the rotating coordinate system.

In the following simulations, three cases are compared. First, the proposed RWDOB and high-gain velocity control were applied to u_y^R to regulate the motion of the end-effector in the y^R direction, while only low-gain velocity control was set on u_x^R to regulate the motion in the x^R direction. This configuration is denoted as "RWDOB on y^R" in the following discussion. Second, the joint space disturbance observer and high-gain velocity control were set on the θ_1 joint, while only low-gain velocity control was set on the θ_2 (i.e., "DOB on θ_1"). Third, the joint space disturbance observer and high-gain velocity control were implemented on the θ_2 joint while only low-gain velocity control was applied to the θ_1 joint (i.e., "DOB on θ_2"). All the simulations were conducted using a commercialized simulation toolbox, Adams/Machineary™. In the simulations, the time constant of the Q filter was set to $\frac{1}{2\pi\cdot 10}$, and the feedback gains were set to form the characteristic polynomial of the closed loop system into a second order system as $s^2+2\xi\omega s+\omega^2$. In the high gain control case, ω was set to 10π rad, and ξ was set to 10, while in the low gain control case, ω was set to 6π rad, and ξ to 4. Two types of the initial posture configurations were used: $\theta_2^0=\frac{\pi}{100}$ and $\theta_2^0=\frac{\pi}{6}$.

In order to evaluate the reaction performance against high-frequency external forces, a 30kg ball collided the tip of the end-effector as shown in Fig. 4, and the reaction against the collision was examined for the aforementioned three cases. The gravity was applied from the left to the right side of figures. An additional link was added at the end-effector to provide a large contact area, and the rotation of the additional link was neglected since its motion is irrelevant here. The other parameters of the manipulator were set the same as Table I.

Figure 4 shows the difference in the reactions between the conventional disturbance observers and the proposed RWDOB. The proposed observer could keep the position of the end-effector in the y^R direction, while the end-effector moved compliantly in the x^R direction. However the conventional observer either reacted rigidly in all the directions [see "DOB on θ_2" in the right figure of Fig. 4(a)] or could not keep the position of the end-effector [see "DOB on θ_1" in the left figure of Fig. 4(a)].

V. CONCLUSION

The rotating coordinate system based on a biarticular actuation mechanism were introduced in this paper. The proposed methods simplified the kinematics, statics, and dynamics of a two-link robotic manipulator. The proposed control algorithm was particularly useful for realizing the dynamic characteristics of a spring-loaded inverted pendulum model. The derivation of dynamic equations in the rotating coordinate system, theoretical analysis, and simulation results were given in this paper, and the simulation results verified the effectiveness of the proposed control algorithm and mechanism.

Although the SLIP model was applied as an application of the proposed algorithm in this paper, it can be applied to any robotic manipulators including robot legs and arms, whose motions consist of the translational motion and the rotational motion.

REFERENCES

[1] F. E. Zajac, R. R. Neptune, and S. a. Kautz, "Biomechanics and muscle coordination of human walking. Part I: Introduction to concepts, power transfer, dynamics and simulations," *Gait & posture*, vol. 16, pp. 215–32, Dec. 2002.

[2] F. E. Zajac, R. R. Neptune, and S. a. Kautz, "Biomechanics and muscle coordination of human walking: part II: Lessons from dynamical simulations and clinical implications," *Gait & posture*, vol. 17, pp. 1–17, Feb. 2003.

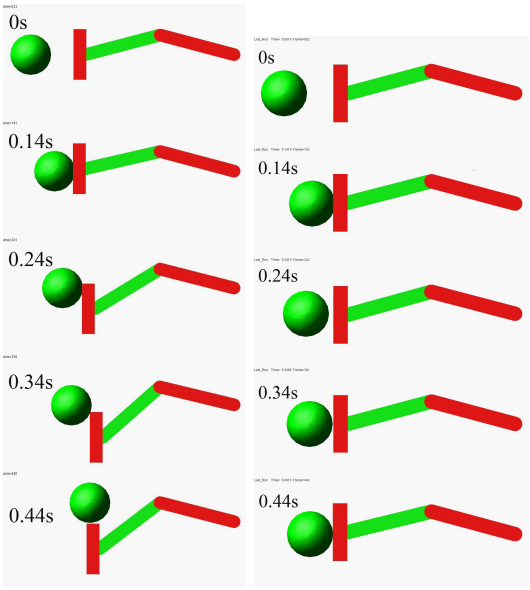

(a) Reactions by the conventional DOB
(Left: DOB on θ_1, Right: DOB on θ_2)

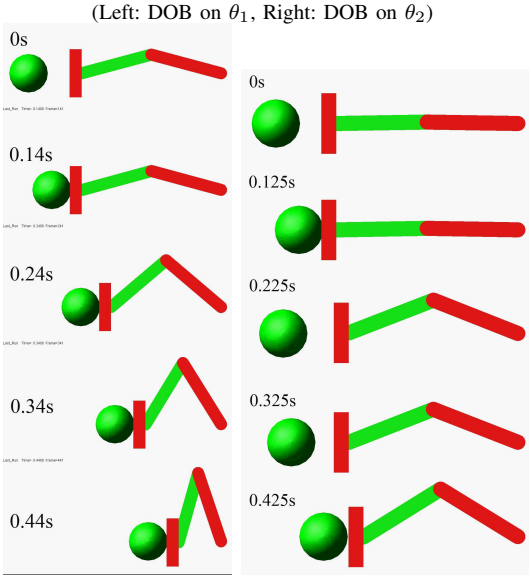

(B) Reactions by the proposed RWDOB (RWDOB on y^R)
(Left: $\theta_2^0 = \frac{\pi}{6}$, Right: $\theta_2^0 = \frac{\pi}{100}$)

Fig. 4. Contact reaction simulation results

[3] G. J. van Ingen Schenau, M. F. Bobbert, and R. H. Rozendal, "The unique action of bi-articular muscles in complex movements.," *Journal of anatomy*, vol. 155, pp. 1–5, Dec. 1987.

[4] M. Kumamoto, "Control properties induced by the existence of antagonistic pairs of bi-articular muscles - Mechanical engineering model analyses," *Human Movement Science*, vol. 13, pp. 611–634, 1994.

[5] S. Oh, V. Salvucci, and Y. Hori, "Development of simplified statics of robot manipulator and optimized muscle torque distribution based on the statics," in *American Control Conference*, pp. 4099 –4104, Jul. 2011.

[6] R. Niiyama, S. Nishikawa, and Y. Kuniyoshi, "Athlete robot with applied human muscle activation patterns for bipedal running," in *Humanoid Robots (Humanoids), 2010 10th IEEE-RAS International Conference on*, pp. 498 –503, Dec. 2010.

[7] J. Hurst, J. Chestnutt, and A. Rizzi, "The actuator with mechanically adjustable series compliance," *Robotics, IEEE Transactions on*, vol. 26, pp. 597 –606, Aug. 2010.

[8] S. Oh, Y. Kimura, and Y. Hori, "Reaction force control of robot manipulator based on biarticular muscle viscoelasticity control," in *Advanced Intelligent Mechatronics, IEEE/ASME International Conference on*, pp. 1105 –1110, Jul. 2010.

[9] J. Craig, *Introduction to robotics: mechanics and control*. Pearson/Prentice Hall, 2005.

[10] M. Spong and S. Hutchinson, *Robot Modeling and Control*. Wiley, 2005.

[11] R. Blickhan, "The spring-mass model for running and hopping," *Journal of Biomechanics*, vol. 22, pp. 1217–1227, Jan. 1989.

[12] H. Geyer, A. Seyfarth, and R. Blickhan, "Compliant leg behaviour explains basic dynamics of walking and running.," *Proceedings. Biological sciences / The Royal Society*, vol. 273, pp. 2861–7, Nov. 2006.

[13] I. Poulakakis and J. Grizzle, "The spring loaded inverted pendulum as the hybrid zero dynamics of an asymmetric hopper," *Automatic Control, IEEE Transactions on*, vol. 54, pp. 1779 –1793, Aug. 2009.

[14] S. Oh and Y. Hori, "Development of two-degree-of-freedom control for robot manipulator with biarticular muscle torque," in *American Control Conference*, pp. 325 –330, Jun. 2009.

[15] T. Tsuji, "A model of antagonistic triarticular muscle mechanism for lancelet robot," in *Advanced Motion Control, IEEE International Workshop on*, pp. 496 –501, Mar. 2010.

[16] T. Umeno and Y. Hori, "Robust speed control of dc servomotors using modern two degrees-of-freedom controller design," *Industrial Electronics, IEEE Transactions on*, vol. 38, pp. 363 –368, Oct. 1991.

[17] Y. Kimura, S. Oh, and Y. Hori, "Leg space observer on biarticular actuated two-link manipulator for realizing spring loaded inverted pendulum model," in *Advanced Motion Control, IEEE International Workshop on*, pp. 1 –6, Mar. 2012.

[18] A. Lasnier and T. Murakami, "Workspace based force sensorless bilateral control with multi-degree-of-freedom motion systems," in *Advanced Motion Control, IEEE International Workshop on*, pp. 583–588, 2010.

[19] T. Umeno, T. Kaneko, and Y. Hori, "Robust servosystem design with two degrees of freedom and its application to novel motion control of robot manipulators," *IEEE Trans. Industrial Electronics*, vol. 40, no. 5, pp. 473–485, 1993.